First-principles investigation of the structural phases and enhanced response properties of the $BiFeO_3$-$LaFeO_3$ multiferroic solid solution

O. E. González-Vázquez, Jacek C. Wojdeł, Oswaldo Diéguez, and Jorge Íñiguez
Institut de Ciència de Materials de Barcelona (ICMAB-CSIC), Campus UAB, 08193 Bellaterra, Spain
(Received 20 December 2011; published 27 February 2012)

We present a first-principles study of the $Bi_{1-x}La_xFeO_3$ (BLFO) solid solution formed by multiferroic $BiFeO_3$ (BFO) and the paraelectric antiferromagnet $LaFeO_3$ (LFO). We discuss the structural transformations that BLFO undergoes as a function of La content and the connection of our results with the existing crystallographic studies. We find that, in a wide range of intermediate compositions, BLFO presents competitive phases that are essentially degenerate in energy. Further, our results suggest that, within this unusual morphotropic region, an electric field might be used to induce various types of paraelectric-to-ferroelectric transitions in the compound. We also discuss BLFO's response properties and show that they can be significantly enhanced by partial substitution of Bi/La atoms in the pure BFO and LFO materials. We analyze the atomistic mechanisms responsible for such improved properties and show that the effects can be captured by simple phenomenological models that treat explicitly the composition x in a Landau-like potential.

DOI: 10.1103/PhysRevB.85.064119 PACS number(s): 77.84.−s, 75.85.+t, 71.15.Mb, 61.50.Ah

I. INTRODUCTION

Magnetoelectric (ME) multiferroics (MFs) are insulators with coupled electric and magnetic orders.[1] Thus, for example, the magnetic properties of these materials can be controlled by means of external electric fields, an uncommon property that makes them very interesting from both fundamental and applied viewpoints.

Perovskite oxide bismuth ferrite ($BiFeO_3$ or BFO) is the best studied compound of this family,[2] as it is one of the few simple crystals that presents ME-MF order at room temperature (T_r). From the applications perspective, one of the current challenges is to enhance BFO's ME couplings at T_r, in particular the linear effect given by the tensor $\boldsymbol{\alpha}$. (In a linear ME material $\Delta\boldsymbol{M} = \boldsymbol{\alpha}\boldsymbol{\mathcal{E}}$, where $\boldsymbol{\mathcal{E}}$ and $\Delta\boldsymbol{M}$ are, respectively, the applied electric field and the field-induced magnetization.) This coupling is not allowed by symmetry in bulk BFO, as the occurrence of an incommensurate cycloid modulation of BFO's antiferromagnetic (AFM) spin structure results in a null macroscopic effect. Moreover, even if the cycloid modulation is lifted—something that can be achieved by partial chemical substitution of the cations[3] and maybe by applying an epitaxial strain[4,5]—both experiments[6,7] and first-principles simulations[8] suggest that BFO's linear ME coupling is relatively weak.

As regards the strategies to increase BFO's ME response, first-principles work[8] indicates that trying to enhance the magnetostructural couplings of the material by replacing Fe with other magnetic species—which, for example, might present stronger spin-orbit interactions—is not a promising route. The calculations show that BFO's response to an electric field is dominated by the deformation of the Bi-O bonds, while the transition-metal ions remain relatively inert. Hence, the magnetic response to $\boldsymbol{\mathcal{E}}$ is an indirect effect that relies on a Bi-dominated structural distortion, and is not strongly dependent on the nature of the magnetic cation.

A more promising route to optimize $\boldsymbol{\alpha}$ consists in bringing the AFM or ferroelectric (FE) ordering temperatures (T_N and T_C, respectively) close to T_r. (For bulk BFO we have T_N = 643 K and $T_C \approx$ 1100 K.[2]) Having $T_N \gtrsim T_r$ would imply a strongly fluctuating spin system at T_r, which should lead to an enhancement of the ME response via the mechanism discussed by Mostovoy *et al.*[9] Having $T_{FE} \gtrsim T_r$ would imply large structural deformations in response to an applied $\boldsymbol{\mathcal{E}}$ field; such a *structural softness* would result in an enhancement of the so-called *lattice-mediated* ME effect,[10] which can be shown to essentially follow the behavior of the dielectric response of the material.[8] Note that, strictly speaking, one expects to obtain a divergence of the lattice-mediated part of $\boldsymbol{\alpha}$ at temperatures close to a second-order FE transition.[11,12]

There are many possible strategies to tune the FE and magnetic ordering temperatures and thus enhance the ME response; for example, one may take advantage of the misfit strain imposed by a substrate on a thin film,[11,13,14] exploit size effects,[13,15] etc. In particular, BFO-based solid solutions seem ideally suited to obtain such enhanced responses, as some chemical substitutions make it possible to tune the nature of the structural transitions of these compounds and the temperature at which they occur. For example, the work of Karpinsky *et al.*[16] with $(BiFeO_3)_{1-x}$-$(CaTiO_3)_x$ has shown that the ME response of the material at T_r can be increased by more than one order of magnitude by adjusting the $CaTiO_3$ content, an effect that the authors attribute to the structural-softness mechanism mentioned above. Also, Kan *et al.*[17] have shown that an enhanced dielectric response is obtained in BFO samples in which Bi is partially substituted by a rare-earth R, with R = Sm, Gd, Dy, etc. Further, these $Bi_{1-x}R_xFeO_3$ compounds present an interesting and seemingly *universal* phase diagram; in particular, at intermediate compositions they exhibit an anomalous response to applied electric fields that has been associated with an $\boldsymbol{\mathcal{E}}$-induced paraelectric (PE)-to-FE transition.

This is the context of our first-principles investigation of a similar and representative material: $Bi_{1-x}La_xFeO_3$ (BLFO), which combines BFO with PE compound $LaFeO_3$ (LFO). BLFO has traditionally attracted interest as it was shown that the spin cycloid characterizing bulk BFO disappears upon doping with La.[3] Presently, the above-described findings in $Bi_{1-x}R_xFeO_3$ solid solutions are bringing renewed attention to

BLFO as well.[18,19] In fact, BLFO appears as the ideal model system to investigate from first principles the physics of these compounds, as it seems to present the same sort of phase diagram and allows for simulations that do not suffer from the potential complications associated with the treatment of rare-earth elements (i.e., f electrons).

Our calculations predict an enhancement of the functional responses of BLFO for compositions close to both the BFO and the LFO limits, revealing the atomistic mechanisms responsible for the improved properties. Further, our results indicate that, for a wide range of intermediate compositions, BLFO presents several (meta)stable phases that are quasidegenerate in energy. Interestingly, the simulations are compatible with the occurrence of $\boldsymbol{\mathcal{E}}$-induced PE-to-FE transitions.

The paper is organized as follows. In Sec. II we describe the simulation methods employed. In Sec. III we present and discuss our results, which are divided into several blocks. In Sec. III A we show the computed phase diagram of $Bi_{1-x}La_xFeO_3$ as a function of the La content x and our results for the x dependence of the structure and ferroelectric polarization of the phases investigated. In Sec. III B we discuss the possibility that field-driven PE-to-FE transitions may occur in the range of intermediate compositions within which we find two quasidegenerate stable phases that coexist. Section III C is devoted to the analysis of the response properties of BLFO for $x \lesssim 1$; we show that the enhancement of the response is the result of a Bi-induced softening of a ferroelectric mode of LFO. In Sec. III D we discuss the enhancement of the response for $x \gtrsim 0$; we show that the effect is related to the large lattice relaxation around the La atoms, which results in an increase in the number of polar modes contributing to the response. In Sec. III E we introduce a simple phenomenological (Landau-like) model that captures and helps us rationalize such effects. Note that in this work we have studied the dielectric response of the material, which is much easier to compute than the ME response and captures the structural-softness-related enhancement that is common to both. In Sec. III F we discuss the connections of our results with the experimental literature on BLFO. Finally, in Sec. IV we give our conclusions.

II. METHODS

For the simulations we used the generalized gradient approximation to density functional theory (more precisely, the so-called "PBE" scheme proposed by Perdew *et al.*[20]) as implemented in the VASP package.[21] As shown in a previous work,[22] the choice of functional has a significant effect on the relative stability of the phases here investigated, and the PBE scheme seems to be the best option to treat the rhombohedral and orthorhombic structures that are relevant for BLFO. A "Hubbard-U" scheme with $U = 4$ eV was used for a better treatment of iron's $3d$ electrons.[23] We used the "projector augmented wave" method to represent the ionic cores,[24] solving for the following electrons: Fe's $3p$, $3d$, and $4s$; Bi's $5d$, $6s$, and $6p$; La's $5s$, $5p$, $5d$, and $6s$; and O's $2s$ and $2p$. Wave functions were represented in a plane-wave basis truncated at 500 eV, and a $3 \times 3 \times 3$ Γ-centered k-point grid was used for integrations within the Brillouin zone (BZ)

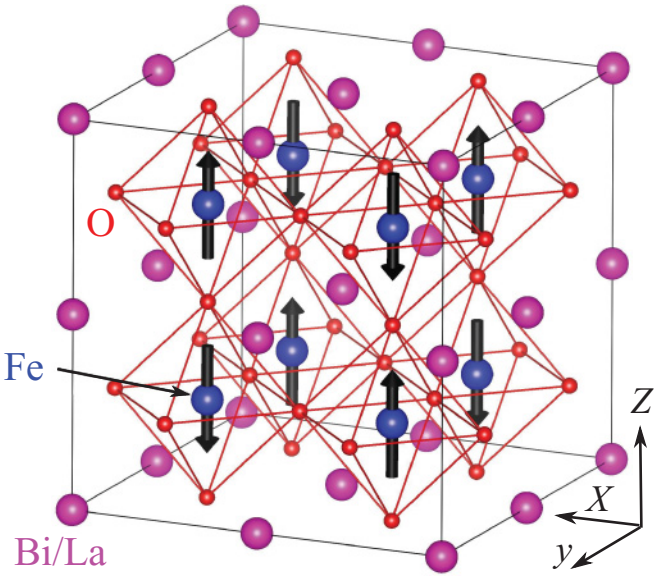

FIG. 1. (Color online) Supercell used in our simulations. The arrows on the Fe ions indicate the G-AFM spin arrangement that characterizes BLFO.

corresponding to the 40-atom cell of Fig. 1. The calculation conditions were checked to render converged results.

We worked with the 40-atom cell depicted in Fig. 1, which is obtained by doubling the five-atom cell of the ideal perovskite structure along the three Cartesian directions, denoted by x, y, and z in the following. This cell is compatible with the experimentally observed atomic structures of BFO [rhombohedral $R3c$ space group and 10-atom primitive cell; sketched in Fig. 2(a) and denoted "R phase" in the following] and LFO [orthorhombic $Pnma$ space group and 20-atom cell; sketched in Fig. 2(b) and denoted "$O1$ phase" in the following], and with the AFM spin arrangement that is common to both (i.e., the so-called G-AFM, with first-nearest-neighboring spins antiparallelly aligned; see Fig. 1). Further, this 40-atom cell captures the structural distortions that characterize the low-symmetry phases of most perovskite oxides[25] and was used in a previous work to identify the most stable phases of BFO.[22] We thus started this project expecting that our simulated system would capture the average unit cell of BLFO for arbitrary x in a realistic way; yet, recent experiments suggest that BLFO's intermediate phases may present even more complex structures that are not compatible with our chosen settings.[18,19] The conclusions of the present work as regards BLFO's morphotropic transitions are thus conditioned by this limitation; this issue is discussed in some detail in Sec. III F.

We conducted a systematic search for stable phases that are likely to be relevant to the BLFO phase diagram. To do this, we followed the procedure described in Ref. 22, which includes consideration of essentially all possible FE and antiferroelectric (AFE) distortions of the cubic perovskite structure, as well as all coherent rotation patterns of the O_6 octahedra. (By *coherent* rotation patterns we mean those expressible in Glazer's notation[25] and combinations of them.) For the structural search, we considered the pure compounds BFO ($x = 0$) and LFO ($x = 1$), as well as the $x = 1/2$

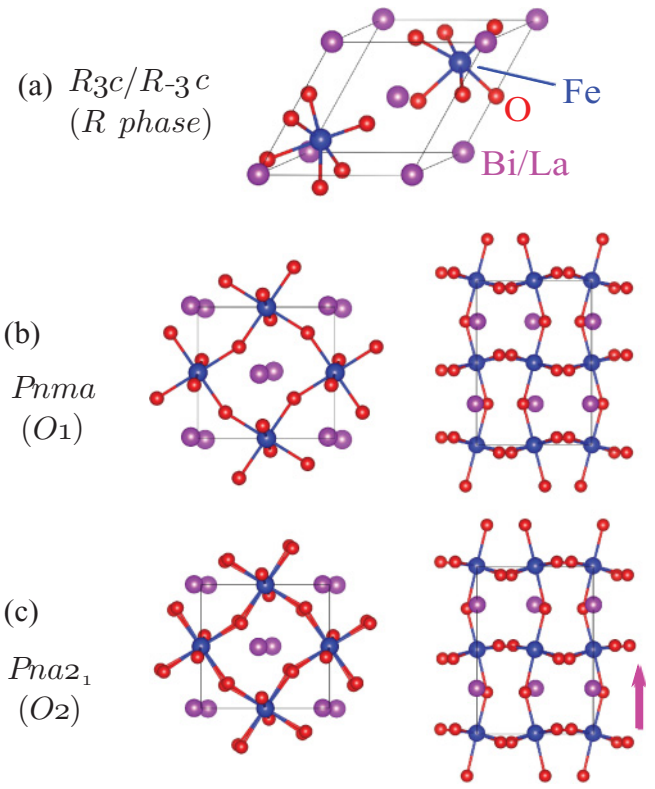

FIG. 2. (Color online) BLFO phases studied in this work. (a) $R3c$ phase that is the ground state of pure BFO. In essence, this structure reduces to $R\bar{3}c$ when the Bi/La and Fe cations locate at the centrosymmetric positions in the middle of their first-neighboring oxygen shells. (b) $Pnma$ structure that is the ground state of pure LFO. (c) $Pna2_1$ structure. The arrow indicates the direction along which a polarization appears driven by the displacement of the Bi/La sublattice. In panels (b) and (c), two views of the unit cell are shown.

composition with a rock-salt arrangement of the Bi/La atoms. The results are described in Sec. III A.

Then, for each of the relevant phases identified we studied all compositions compatible with our 40-atom cell, which allows us to vary the La content in steps $\Delta x = 1/8$. At intermediate values of x, the effect of the substitutional disorder was studied by simulating explicitly *all* inequivalent Bi/La arrangements. For all the BLFO configurations investigated, the atomic structure was fully relaxed until residual forces and stresses become smaller than 0.01 eV/Å and about 1 kB, respectively; selected cases were further considered for the computation of their electric polarization and electromechanical response properties, following standard methods.[26] In all cases we worked with the G-AFM magnetic order.

III. RESULTS AND DISCUSSION

A. Phase diagram and basic properties

The phase diagram of BLFO as a function of the La content has been studied by a number of authors,[3,18,19,27–30] but the results are often incomplete and even contradictory with each other, and a clear picture of the phases at intermediate compositions is yet to emerge. Hence, we started this work by searching for likely candidates.

We identified three phases that may be relevant to the phase diagram of BLFO: the ground-state configurations of BFO [Fig. 2(a)] and LFO [Fig. 2(b)] already mentioned above, as well as a structure that is ferroelectric and presents the $Pna2_1$ space group. This third phase, which is sketched in Fig. 2(c) and denoted "$O2$ phase" in the following, is similar to LFO's orthorhombic ground state: It presents the same unit cell and O_6-rotation pattern (i.e., antiphase rotations around the $[110]_{pc}$ pseudocubic direction and inphase rotations around $[001]_{pc}$, denoted by $a^-a^-c^+$ in Glazer's notation[25]). Additionally, it displays a relatively large spontaneous polarization along $[001]_{pc}$; we obtained a maximum value of about 0.5 C/m^2 for the $O2$ structure with the BFO composition, which is comparable with the large polarization (about 0.9 C/m^2) of BFO's FE ground state. Note also that, in the $O2$ phase, such a polarization coexists with an antipolar pattern of Bi displacements within the $(001)_{pc}$ plane.

Figure 3(a) shows the formation energy of the investigated phases as a function of composition; this is defined as $E_{for} = E - (1-x)E_{BFO} - xE_{LFO}$, where E is the energy of

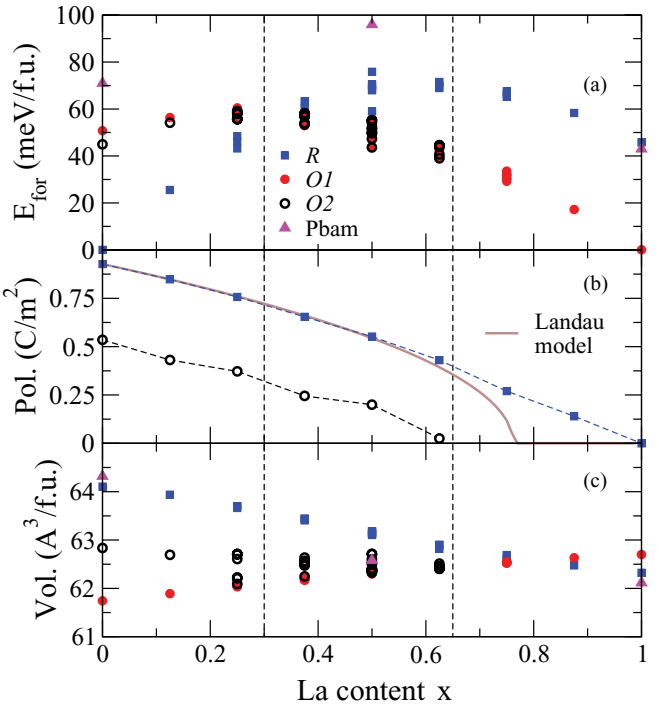

FIG. 3. (Color online) (a) Formation energy of the three phases investigated as a function of composition (see text). For a given color and composition, each point in the figure corresponds to a different arrangement of the Bi/La atoms. The magenta triangles correspond to the $PbZrO_3$-like $Pbam$ phase discussed in Sec. III F. (b) Polarization of the R and $O2$ phases as a function of composition, computed for representative Bi/La arrangements. The solid line is the result of the Landau model discussed in Sec. III E. Dashed lines are guides to the eye. (c) Cell volume per five-atom formula unit for all phases and Bi/La arrangements [as in panel (a)]. In all panels, the two dashed vertical lines mark, respectively, the discontinuous transformation between R and O phases (at $x \approx 0.3$) and the loss of stability of the $O2$ structure (at $x \approx 0.65$).

a particular BLFO structure of composition x, and E_{BFO} and E_{LFO} are the ground-state energies of the pure compounds. Note that, at a given x, several points may appear for one particular phase; each one of them corresponds to a different Bi/La arrangement. Figure 3 also shows the polarization of selected structures [panel (b)] and the volume per formula unit [panel (c)].

Our results indicate that the R phase of bulk BFO is the most stable structure for $x \lesssim 0.3$. At $x \approx 0.3$, we predict a discontinuous transition [e.g., see in Fig. 3(c) the sharp change in the volume *per* formula unit that is expected to occur] to a denser orthorhombic structure that could be either $O1$ or $O2$. The computed energy gap between $O1$ and $O2$ is smaller than the dispersion associated to having different Bi/La arrangements; hence, our results indicate that these two phases are essentially as stable within the $0.3 \lesssim x \lesssim 0.65$ range. For $x \gtrsim 0.65$, we find that the $O2$ phase loses its stability; our structural relaxations starting from the $O2$ structure recover the $O1$ solution for all Bi/La arrangements. It is not possible for us to study in detail the transition by which $O2$ destabilizes for increasing x, as we are limited to $\Delta x = 1/8$ composition steps. Nevertheless, let us note that our results clearly rule out a second-order transformation between $O1$ and $O2$, as we explicitly verified that (i) the $O1$ phase is a local minimum of the energy for all compositions (i.e., it is stable against any combination of atomic and cell distortions compatible with our 40-atom cell) and (ii) the $O2$ phase is local minimum of the energy for $x \leqslant 5/8$.[31] The simultaneous stability of these two phases and the possibilities it may open are further discussed in Sec. III B.

Figure 3(b) shows how the spontaneous polarization of BLFO's R phase decreases as the La content increases, disappearing at $x = 1$. In fact, in that limit the R phase becomes paraelectric, presenting the $R\bar{3}c$ rhombohedral space group. A decreasing polarization for increasing x is also observed for the $O2$ phase. We inspected our relaxed structures for both cases and found the origin of this behavior: In essence, our results indicate that La^{3+} tends to prefer oxygen environments that are relatively isotropic and highly coordinated; this contrasts with the large off-centering and anisotropic oxygen environments that are usual for Bi^{3+}, which are typically explained in terms of a lone-pair mechanism.[22] Interestingly, Bi's chemical preference results in the occurrence of large local electric dipoles (which add up to form the macroscopic polarization), while there is no such local dipole for the ideal La environments (i.e., those observed for LFO's $O1$ ground state as well as for its R-type PE phase of $R\bar{3}c$ symmetry).

B. $\mathcal{E}$-field-driven PE-to-FE transitions

The predicted coexistence of BLFO's $O1$ and $O2$ phases in a wide composition range, and the fact that these two phases are almost exactly as stable, is an uncommon and very suggestive result. Such a coexistence is best appreciated in Fig. 4(a): There we show the energy as a function of the structural distortion that interpolates between the PE $O1$ phase and two $O2$ structures with opposite polarizations. (We quantify the distortion in units of polarization assuming that a linear relationship between its amplitude and P_z.) This calculation was done for $x = 3/8$ and a quasi-rock-salt Bi/La arrangement, which is a representative case. (For the sake of the discussion below, we picked an example in which the PE phase is more stable than the FE phase. Similar triple wells, but with a reversed $O1$-$O2$ stability, were also obtained for different compositions or Bi/La arrangements.)

We can fit the energy vs polarization data of Fig. 4(a) to a sixth-order Landau-like potential of the form

$$F(P_z,\mathcal{E}_z) = F_0 + \tfrac{1}{2}AP_z^2 + \tfrac{1}{4}BP_z^4 + \tfrac{1}{6}CP_z^6 - P_z\mathcal{E}_z. \quad (1)$$

We take $F_0 = 0$ and obtain $A = 7.105 \times 10^8$ Jm/C^2, $B = -4.111 \times 10^{10}$ Jm^5/C^4, and $C = 4.760 \times 10^{11}$ Jm^9/C^6, all expressed in SI units. (To compute these coefficients, we assumed that the volume per elementary perovskite cell is approximately constant and equal to 62.2 Å^3 throughout the interpolation path.) Then we can compute P_z as a function of

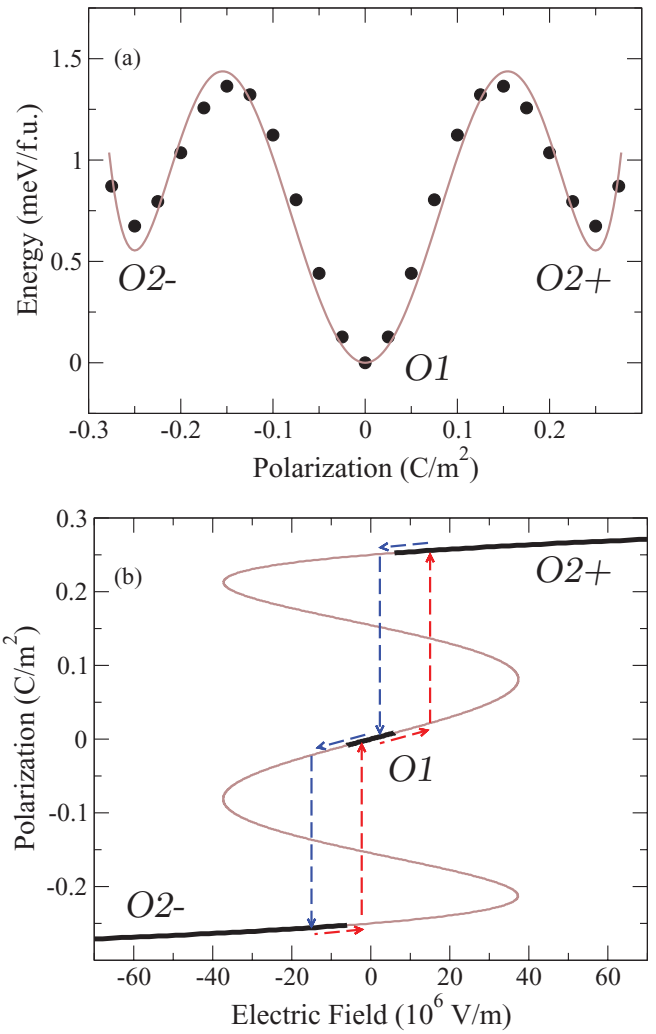

FIG. 4. (Color online) (a) Energy variation along the path interpolating between the $O1$ and $O2$ phases obtained for a particular composition ($x = 3/8$) and Bi/La arrangement. The points correspond to energies obtained from first principles, and the line is a fit to a sixth-order Landau-like potential (see text). (b) Polarization as a function of electric field, as obtained from the fitted Landau-like potential. Thicker lines mark the lowest-energy state. Dashed arrows sketch the transitions between the PE and the FE phases that would occur in a hysteresis cycle.

$\mathcal{E}_z$ and plot the ideal polarization-switching cycle of Fig. 4(b). (We call it *ideal* as we are assuming a monodomain situation and, thus, a switching that occurs homogeneously throughout the material. This is sometimes referred to as the *Landau limit* for polarization switching.) Note that the thick line in Fig. 4(b) indicates the most stable polarization state, and the dashed vertical arrows suggest the hysteresis that one expects to observe when a system transforms discontinuously from a metastable to a stable phase.

This result is strongly reminiscent of the hysteresis loops measured by Kan *et al.* in $Bi_{1-x}R_xFeO_3$ compounds (see Fig. 5 of Ref. 17) and the field-driven PE-to-FE transition hypothesized in that work.[32] Indeed, in accordance with the interpretation of Kan *et al.*, our calculations indicate that, for $x \gtrsim 0.3$, an electric field could be used to make BLFO transform between metastable phases of orthorhombic ($O1$ or $O2$) and rhombohedral (FE R) symmetries. Additionally, as discussed above, our results suggest that in BLFO one might be able to observe a second type of $\mathcal{E}$-driven transformation involving PE $O1$ and FE $O2$ structures; such a transition might, in principle, occur in a rather wide ($0.3 \lesssim x \lesssim 0.65$) composition range.

C. Enhanced response in Bi-doped $LaFeO_3$

Let us now focus on the response properties of the pure compounds and study how they get affected upon substitution of a small fraction of the Bi/La cations. It is convenient to begin with the case of LFO.

Table I shows the computed lattice-mediated part of the dielectric tensor ($\boldsymbol{\chi}^{\text{latt}}$) of LFO and $Bi_{1/8}La_{7/8}FeO_3$ in their ground state ($O1$ phase), as well as a characteristic result for an intermediate ($x = 1/2$) composition. It is apparent that, upon Bi doping, a significant increase of the response occurs for the zz component. We have checked that this effect relies on a low-energy (soft) distortion that is dominated by Bi and essentially identical to the one connecting the PE $O1$ structure with the FE $O2$ phase. In fact, we observed that, for some particular compositions and Bi/La arrangements, this Bi-related soft mode becomes barely stable—which results in very large calculated responses as the one reported in Table I for rock-salt-ordered $Bi_{1/2}La_{1/2}FeO_3$—or even unstable.[31] It is thus trivial to pinpoint the mechanism by which substituting La by Bi enhances the response: The presence of Bi results in the occurrence of a soft mode associated with the development of a polarization along the z direction.

To make this argument more quantitative, let us recall that the lattice-mediated part of the dielectric response is given

TABLE I. Computed dielectric susceptibility tensors for $LaFeO_3$, $Bi_{1/8}La_{7/8}FeO_3$, and $Bi_{1/2}La_{1/2}FeO_3$ (with rock-salt-ordered Bi/La cations) in the $O1$ phase (see text). Results given in the Cartesian (pseudocubic) setting defined in Fig. 1.

	$LaFeO_3$	$Bi_{1/8}La_{7/8}FeO_3$	$Bi_{1/2}La_{1/2}FeO_3$
$\boldsymbol{\chi}^{\text{latt}}$	$\begin{bmatrix} 27 & 0 & 0 \\ 0 & 27 & 0 \\ 0 & 0 & 27 \end{bmatrix}$	$\begin{bmatrix} 35 & 0 & 0 \\ 0 & 37 & 0 \\ 0 & 0 & 39 \end{bmatrix}$	$\begin{bmatrix} 81 & -29 & -82 \\ -29 & 83 & 83 \\ -82 & 83 & 1186 \end{bmatrix}$

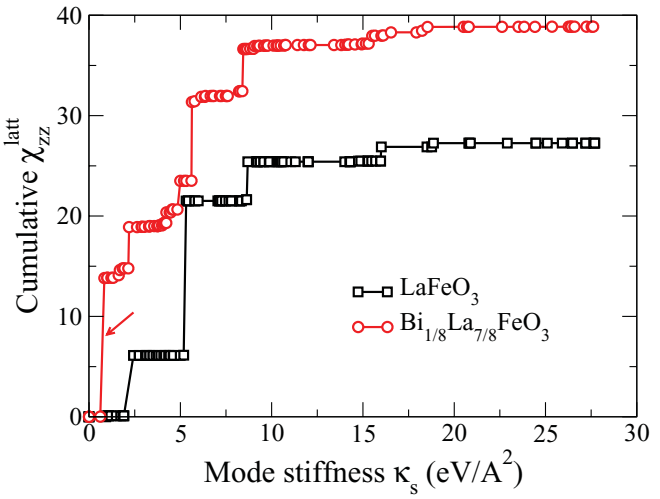

FIG. 5. (Color online) Cumulative plot of the χ_{zz}^{latt} component of the dielectric susceptibility tensor (see text) for the the $O1$ phase of pure $LaFeO_3$ and $Bi_{1/8}La_{7/8}FeO_3$.

by[26]

$$\chi_{\alpha\beta}^{\text{latt}} = \Omega_0^{-1} \sum_{mn} Z_{m\alpha} (K^{-1})_{mn} Z_{n\beta}, \tag{2}$$

where m and n label the displacements of the atoms in the unit cell (which are assumed to be repeated homogeneously throughout the crystal, as corresponding to Γ-point distortions), K_{mn} is the so-called force-constant matrix (i.e., the matrix of second-derivatives of the energy with respect to atomic displacements), $Z_{m\alpha}$ are the atomic Born effective charges (which quantify the polarization change associated to a displacement), and Ω_0 is the unit cell volume at equilibrium.

The existence of a soft mode implies that the $\boldsymbol{K}$ matrix presents a small eigenvalue κ_s, which may result in a large dielectric response. (The dynamical matrix is obtained by appropriately mass scaling $\boldsymbol{K}$; thus, the eigenmodes of both matrices are closely related, and a small κ_s corresponds to a small normal-mode frequency.) This is better appreciated if we write $\boldsymbol{\chi}^{\text{latt}}$ as a sum over $\boldsymbol{K}$ eigenmodes in the following way:

$$\chi_{\alpha\beta}^{\text{latt}} = \frac{1}{\Omega_0} \sum_s \frac{\bar{Z}_{s\alpha} \bar{Z}_{s\beta}}{\kappa_s}, \tag{3}$$

where $\bar{Z}_{s\alpha}$ are the mode effective charges, that is, $\bar{Z}_{s\alpha} = \sum_m Z_{m\alpha} \hat{\xi}_{sm}$ with $\hat{\xi}_{sm}$ being the sth eigenvector. In Eq. (3), s runs over all the Γ-point modes that have a nonzero effective charge; these are the so-called *polar* or *infrared active* modes.

By virtue of the mode-by-mode decomposition of Eq. (3), we can make the cumulative plots shown in Fig. 5 and thus analyze the enhancement of χ_{zz}^{latt}. In this case, the situation is very simple: A soft mode (indicated with an arrow in the figure) appears upon the doping with Bi and this single mode produces most of the enhancement. By inspecting the mode eigenvector, we found that it is clearly dominated by a Bi-O distortion. We can thus conclude that the presence of Bi results in a soft polar mode that, in turn, leads to an enhanced dielectric response.

D. Enhanced response in La-doped $BiFeO_3$

Let us now consider the case in which we replace Bi with La in BFO's R phase. Table II shows the χ^{latt} tensors computed for the R phases of pure BFO and $Bi_{7/8}La_{1/8}FeO_3$. A significant isotropic enhancement of the response is clearly appreciated.

We can understand the origin of this enhancement by inspecting the cumulative plots shown in Fig. 6. It is clear that, in this case, the enhancement is not driven by a single soft mode; instead, it relies on the appearance of many new polar modes, each of which gives a small contribution to the response (note the quasicontinuous growth of the cumulative response of $Bi_{7/8}La_{1/8}FeO_3$ in the stiffness range from 0 eV/Å to about 10 eV/Å). Let us stress that these modes are not polar in the R phase of pure BFO, but they acquire a small nonzero polarity when we introduce La in the lattice. Figure 6 also shows the *filtered* response of BFO and $Bi_{7/8}La_{1/8}FeO_3$, obtained by excluding from the sum in Eq. (3) those modes whose polarity is small (i.e., to produce this figure we removed those with $\bar{Z}_{sz} < 2|e|$, where $|e|$ is the elemental charge). In the case of pure BFO, the filtered response is almost identical to the result including all the modes; in contrast, the filtered response of $Bi_{7/8}La_{1/8}FeO_3$ is significantly smaller than the real one, and the La-induced enhancement disappears completely.

Why do we obtain so many new polar modes by doping the BFO-R phase with La? Why did we not find a similar effect when substituting La by Bi in the LFO-$O1$ structure? To understand the reasons for this differentiated behavior, note that pure LFO does *not* present a stable FE phase of $R3c$ symmetry; indeed, as mentioned in Sec. III A, the BLFO's R phase transforms continuously from FE $R3c$ to PE $R\bar{3}c$ as the La content increases. Structurally, such a transformation essentially involves a relocation of the A-site cation: La tends to place itself at a centrosymmetric position, in contrast with Bi's strong off-centering. When placed in the BFO-R structure, the La dopant tries to adopt its preferred configuration, which involves a large local distortion and, thus, a strong symmetry breaking; as a result, many modes that are not polar in the R phase of pure BFO acquire a small nonzero polarity. Such modes respond to the applied field and render a significantly enhanced response. The magnitude of the La-induced symmetry breaking can be better appreciated in the structural data of Table III and the sketch of Fig. 7. In contrast, when we place Bi in the LFO-$O1$ structure, the symmetry breaking is not so dramatic and there is no significant enhancement of the response associated to it. This is consistent with the fact that pure BFO presents a stable $O1$ phase that is structurally very similar to LFO's ground state (see the structural information in Table III and Fig. 7).

TABLE II. Computed dielectric susceptibility tensors for $BiFeO_3$ and $Bi_{7/8}La_{1/8}FeO_3$ in the R phase (see text). Results given in the Cartesian (pseudocubic) setting defined in Fig. 1.

	$BiFeO_3$	$Bi_{7/8}La_{1/8}FeO_3$
χ^{latt}	$\begin{bmatrix} 31 & -5 & -5 \\ -5 & 31 & -5 \\ -5 & -5 & 31 \end{bmatrix}$	$\begin{bmatrix} 39 & -7 & -7 \\ -7 & 39 & -7 \\ -7 & -7 & 39 \end{bmatrix}$

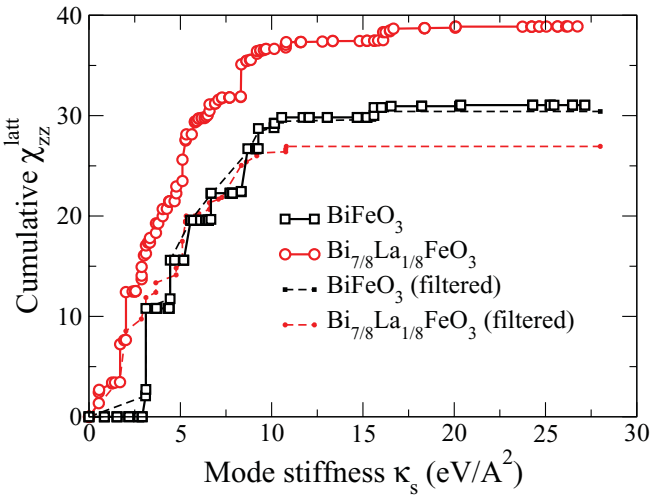

FIG. 6. (Color online) Cumulative plot of the χ^{latt}_{zz} component of the dielectric susceptibility tensor (see text) for the the R phase of pure $BiFeO_3$ and $Bi_{7/8}La_{1/8}FeO_3$.

E. Phenomenological modeling of the response

Let us now discuss how we can capture the response enhancements discussed in Secs. III C and III D by means of Landau-like potentials that include compositional effects explicitly.[33] We also comment on how to interpret such a phenomenological description, emphasizing that the connection with the atomistic picture may be a subtle one.

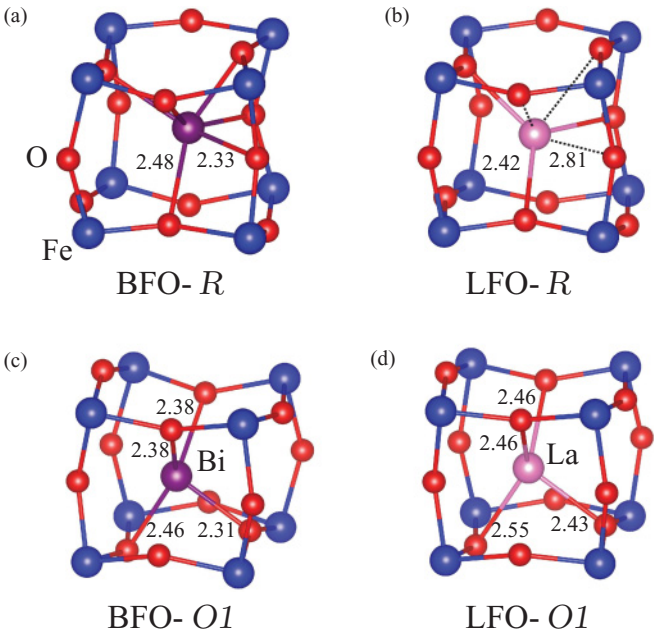

FIG. 7. (Color online) Atomic structure of the R [(a) and (b)] and $O1$ [(c) and (d)] phases of BFO [(a) and (c)] and LFO [(b) and (d)], focusing on the coordination of the A-site cations Bi and La. Representative Bi-O and La-O bond distances (Å) are indicated. In panel (b), dotted lines indicate the three La-O pairs corresponding to the Bi-O bonds of 2.33 Å shown in panel (a).

TABLE III. Computed structures of the R and $O1$ phases of the pure compounds $BiFeO_3$ and $LaFeO_3$. Note that the R phase has space group $R3c$ for BFO and $R\bar{3}c$ for LFO (both given in the primitive representation), while the $O1$ phase has $Pnma$ symmetry for both compounds. As regards the $Pnma$ phases, note that the second (longest) lattice vector of the structures in this table corresponds to the z pseudocubic direction discussed in the text.

$BiFeO_3$ $R3c$		$a=b=c=5.699$ Å $\alpha=\beta=\gamma=59.14^\circ$		
Atom	Wyc.	x	y	z
Bi	2a	0.2217	0.2217	0.2217
Fe	2a	0.0000	0.0000	0.0000
O	6b	0.6849	0.8327	0.2848
$LaFeO_3$ $R\bar{3}c$		$a=b=c=5.570$ Å $\alpha=\beta=\gamma=60.89^\circ$		
Atom	Wyc.	x	y	z
La	2a	1/4	1/4	1/4
Fe	2b	0	0	0
O	6e	0.6789	0.8211	1/4
$BiFeO_3$ $Pnma$		$a=5.719$ Å, $b=7.868$ Å, $c=5.488$ Å $\alpha=\beta=\gamma=90^\circ$		
Atom	Wyc.	x	y	z
Bi	4c	−0.0516	1/4	−0.0095
Fe	4b	0	0	1/2
O	4c	0.5296	1/4	0.0968
O	8d	0.8006	−0.0472	0.1955
$LaFeO_3$ $Pnma$		$a=5.656$ Å, $b=7.929$ Å, $c=5.592$ Å $\alpha=\beta=\gamma=90^\circ$		
Atom	Wyc.	x	y	z
La	4c	−0.0383	1/4	−0.0079
Fe	4b	0	0	1/2
O	4c	0.5187	1/4	0.0775
O	8d	0.7881	−0.0414	0.2124

We write the Landau potential for a single polarization component P as

$$F(P,x,\mathcal{E}) = F(x) + \tfrac{1}{2}AP^2 + \tfrac{1}{4}BP^4 + \tfrac{1}{2}\lambda x P^2 - \mathcal{E}P. \quad (4)$$

Here $F(x)$ contains all constant or P-independent terms; in addition, we have included the lowest-order composition-dependent effects in a way that is analogous to the treatment of temperature in the usual Landau models. [In the case of a disordered solid solution, the composition x is a fully symmetric scalar variable; hence, deducing the symmetry-invariant x terms that can appear in $F(P,x,\mathcal{E})$ is a trivial task.]

In the case of Bi-doped LFO, we are interested in the description of the $O1$ phase, which is paraelectric; thus, we can assume $A>0$ and neglect the fourth-order term B. Further, it is convenient to use $x'=1-x$ as the compositional variable, with $x'=0$ corresponding to pure LFO. Then, the x'-dependent dielectric susceptibility is given by

$$\chi = \frac{1}{A-\lambda x'}. \quad (5)$$

If we use this expression to fit the results for χ_{zz} given in Table I—that is, for $x'=0$ (LFO) and $x'=1/8$ ($Bi_{1/8}La_{7/8}FeO_3$)—we obtain $A=4.178\times10^9$ Jm/C^2 and $\lambda=1.468\times10^9$ Jm/C^2. The positive λ reflects the lattice softening caused by the Bi dopant, which we know from our atomistic simulations is associated with an incipient Bi-driven FE instability. Hence, the application and interpretation of our Landau-like model is straightforward in this case.[34]

This exercise becomes more interesting in the case of La-doped BFO. There we are dealing with the properties of the FE R phase, and we need to consider all the terms in Eq. (4), with $A<0$ and $B>0$. Hence, the equilibrium polarization is given by

$$P_{\rm eq} = \sqrt{-\frac{A+\lambda x}{B}}, \quad (6)$$

and the dielectric response is

$$\chi = -\frac{1}{2(A+\lambda x)}. \quad (7)$$

We fitted the parameters by demanding that the model reproduces correctly (i) $P_{\rm eq}$ for $x=0$ and $x=1/8$ (where P is the modulus of the $[111]_{\rm pc}$-oriented polarization of the R phase) and (ii) the response to a $[111]_{\rm pc}$-oriented electric field at $x=0$. (We checked that alternative fitting strategies—e.g., demanding that the response is reproduced exactly for $x=0$ and $x=1/8$—give very similar results.) The parameters thus computed are $A=-1.818\times10^9$ Jm/C^2, $B=2.247\times10^9$ Jm^5/C^4, and $\lambda=2.375\times10^9$ Jm/C^2. In this case, the obtained positive λ captures two effects: For increasing La content, $P_{\rm eq}$ decreases and χ increases. This makes good physical sense: As x increases, the FE instability weakens and the associated energy well becomes shallower; consequently, it is energetically less costly to act on the polarization of the material, which results in a large dielectric response.

That a weaker FE instability may lead to larger responses is not a new notion; indeed, similar ideas have been proposed to engineer superlattices with large electromechanical responses,[35] and there is a clear connection with the behavior of quantum paraelectrics that, like $SrTiO_3$ and related materials, are very good dielectrics.[36,37] Nevertheless, it is worth noting our atomistic simulations show that the physical underpinnings of this effect are rather subtle in the case of La-doped BFO. Here the shallowness of the FE energy minimum is not caused by a softening of the interatomic interactions, but by the presence of an increased number of infrared active modes resulting from the large distortion of the BFO lattice caused by the La dopant. Thus, this example shows that complex atomistic mechanisms may hide behind Landau potentials whose interpretation might seem straightforward.

Finally, let us note that our Landau-like potential for BLFO's R phase allows us to predict the behavior of $P_{\rm eq}$ in a wide range of compositions [see the solid line in Fig. 3(b)].[38] This is remarkable, taking into account that the potential parameters were fitted to reproduce results obtained in the limit of pure BFO. Hence, this seems to be a new example of how Landau potentials are often accurate well outside its expected range of applicability; this fact has been pointed out by other authors as regards the modelization of temperature-dependent

properties,[39] and our work suggests that the same is true in the case of a varying composition.

F. Connection with experiment

Many of the experimental works on BLFO have found a large number of structural transitions as a function of composition, and intermediate phases of orthorhombic, monoclinic, and triclinic symmetries,[3,19,27,28] and even incommensurate structures,[18] have been reported. Further, physical characterization of the BLFO samples has also provided evidence for several phase transitions.[27,40] Yet, most reports disagree on the exact number of transitions and the character of the intermediate phases. In this respect, our results suggest that some of the symmetries proposed in the literature may not correspond to stable BLFO structures. More precisely, some of the published phases (e.g., the $C222$ and $C222_1$ variants reported by Zalesskii *et al.*,[3] or the $Imma$ symmetry reported by Troyanchuk *et al.*[30]) should be compatible with the simulation cell considered in this work; yet, in our structural search we did not find any local energy minimum with such symmetries.

Recently, Troyanchuk *et al.*[19] conducted a careful study—especially in what regards the preparation of the BLFO samples—and found a different intermediate phase at $x \approx 0.18$. That phase has a $Pbam$ space group, and is similar to the ground-state structure of PE perovskite $PbZrO_3$; in particular, it presents an orthorhombic-shaped 40-atom primitive cell that is incompatible with the pseudocubic simulation box considered here. (Such a cell is usually described as a $\sqrt{2}a \times 2\sqrt{2}a \times 2a$ repetition of the elemental perovskite unit, while our simulation cell would be a $2a \times 2a \times 2a$ repetition.) We have run a first-principles study to determine the formation energy of this $PbZrO_3$-like phase, using the crystallographic data provided in Ref. 19 as starting point of our structural relaxations. We have considered three different compositions (i.e., pure BFO, pure LFO, as well as $Bi_{1/2}La_{1/2}FeO_3$ with a rock-salt arrangement of the Bi and La atoms) and the usual G-AFM spin arrangement. The results are shown in Figs. 3(a) and 3(c) as magenta triangles: We find that the phase proposed by Troyanchuk *et al.* is metastable at all the compositions considered.[41] Further, it always lies above the $O1$ structure and its formation energy is rather high at compositions that are rich in Bi. Hence, our results seem to suggest that this phase is not likely to appear in BLFO's phase diagram.

Hence, except for the stable phases of the pure compounds ($R3c$ for BFO and $Pnma$ for LFO), our first-principles calculations do not support any of the many structures that have been found experimentally in BLFO's phase diagram. Of course, we must note that our simulations do not include thermal effects and are restricted to the investigation of local energy minima; in contrast, the real materials may present, at finite temperatures, stable phases that are not minima of the potential energy. Hence, our conclusions are not definitive. Nevertheless, noting that, in the case of pure BFO, all the structures appearing in its phase diagram seem to be local energy minima,[22] it is somewhat surprising that we were not able to validate with our simulations any of the intermediate phases observed experimentally in BLFO.

Our results suggest a possible explanation for the diversity of structural phases found in this compound. The positive formation energies shown in Fig. 3(a) indicate that there is an energy cost associated with the stabilization of the BLFO solid solution; in other words, at all compositions the most thermodynamically stable configuration would involve a phase separation in BFO-R and LFO-$O1$. That the solid-solved phase of these complex oxides is thermodynamically unstable is not a new notion; for example, some of us have obtained results leading to similar conclusions for the compounds $BiFeO_3$-$BiCoO_3$ [see Fig. 1(a) of Ref. 42, which summarizes the outcomes of a study analogous to the present one], $PbZrO_3$-$PbTiO_3$, and $BiScO_3$-$PbTiO_3$ (see Fig. 2 of Ref. 43, from which the formation energy can be easily derived; note that in this case the calculations were performed using the so-called virtual-crystal approximation). The predicted instability of BLFO's solid-solved phase clearly indicates that it may be a hard task to prepare samples in which the Bi and La atoms are well disordered. In fact, in many of the crystallographic works it was necessary to assume some sort of phase coexistence to model the structural data at intermediate compositions, and Troyanchuk *et al.*[19] have described how the sample-preparation procedure can critically affect the results. All these facts suggest that most of the BLFO phases reported in the literature do probably occur in samples prepared in some specific conditions; yet, it is not so clear whether they may be stable phases of an ideal solid solution with Bi/La disorder.

Along the same lines, let us note that the difficulties to identify BLFO's most stable phase pertain to compositions in the $0.1 \lesssim x \lesssim 0.5$ range. Again, this seems consistent with our calculations, as that is the region in which (i) we find the crossover from the R phase to the orthorhombic structures $O1$ and $O2$, and (ii) according to our results BLFO can adopt different orthorhombic conformations that are essentially degenerate in energy.

IV. SUMMARY AND CONCLUSIONS

We have used first-principles methods to study the $Bi_{1-x}La_xFeO_3$ (BLFO) solid solution formed by multiferroic $BiFeO_3$ (BFO) and the paraelectric antiferromagnet $LaFeO_3$ (LFO). We have investigated BLFO's phase transitions as a function of the La content x. We find that at $x \approx 0.3$ BLFO transforms discontinuously from BFO's rhombohedral ferroelectric phase into an orthorhombic structure. The nature of such an orthorhombic phase could not be fully determined from the simulations, as we obtained two different states—namely, ferroelectric $Pna2_1$ and paraelectric $Pnma$—that are essentially as stable in the $0.3 \lesssim x \lesssim 0.65$ composition range. We find that the paraelectric $Pnma$ phase prevails for $x \gtrsim 0.65$.

Such a phase coexistence at intermediate x values suggests some appealing possibilities; for example, our results indicate that an electric field might be used to induce paraelectric-to-ferroelectric phase transformations in this compound. We have also discussed the connection between our results and published crystallographic studies of BLFO solid solutions, noting that our simulations do not support any of the many different phases that have been experimentally proposed to

occur at intermediate compositions. Our results suggest some explanations for the experimental difficulties that hamper BLFO's structural characterization.

Additionally, we have shown that the chemical substitution of Bi/La atoms in the pure compounds leads to significantly improved response properties. (Our calculations were restricted to the dielectric susceptibility, and we argue that the obtained enhancement should be observed in the ME response as well.) We have analyzed in detail the diverse origins of the increased responses. In the case of Bi-doped LFO, the enhancement is associated with an incipient ferroelectric instability involving Bi-O distortions. In contrast, in La-doped BFO the improvement relies on the strong structural relaxation and local symmetry breaking caused by the La atoms, which result in the appearance of many new polar modes that react to an applied electric field. We have shown that both effects can be captured by a phenomenological theory in which the composition x is explicitly treated in a Landau-like potential.

In conclusion, our first-principles results for the BLFO multiferroic solid solution suggest that these compounds present many appealing features, ranging from improved response properties to the possibility of inducing structural phase transitions by application of electric fields. Further, we find that several BLFO phases are quasidegenerate in energy in a wide composition range; thus, our calculations suggest that BLFO undergoes a very unusual morphotropic transformation that deserves a detailed experimental investigation. Finally, some of our results are strongly reminiscent of phenomena that has been experimentally found in similar solid solutions, as for example the $Bi_{1-x}R_xFeO_3$ compounds where R is a rare-earth lanthanide; such similarities suggest that BLFO may be a convenient model system representative of this larger family of materials. Hence, we hope our work will contribute to a better understanding of BLFO and related compounds, and to bring renewed attention to such promising multiferroics.

ACKNOWLEDGMENTS

This work was supported by MICINN-Spain [Grants No. MAT2010-18113, No. MAT2010-10093-E, and No. CSD2007-00041; and the Ramón y Cajal program (O.D.)], the EC-FP7 project OxIDes (Grant No. CP-FP 228989-2), and CSIC's JAE-pre (O.E.G.V.) and JAE-doc (J.C.W.) programs. We used supercomputing facilities provided by RES and CESGA. Fruitful discussions with L. Bellaiche and J. M. Pérez-Mato are gratefully acknowledged.

[1] M. Fiebig, J. Phys. D: Appl. Phys. **38**, R123 (2005).
[2] G. Catalan and J. F. Scott, Adv. Mater. **21**, 2463 (2009).
[3] A. V. Zalesskii, A. A. Frolov, T. A. Khimich, and A. A. Bush, Phys. Sol. St. **45**, 141 (2003).
[4] H. Béa, M. Bibes, S. Petit, J. Kreisel, and A. Barthélémy, Phil. Mag. Lett. **87**, 165 (2007).
[5] W. Ratcliff III, D. Kan, W. Chen, S. Watson, S. Chi, R. Erwin, C. J. McIntyre, S. C. Capelli, and I. Takeuchi, Adv. Funct. Mater. **21**, 1567 (2011).
[6] Y. F. Popov, A. K. Zvezdin, G. P. Vorobev, A. M. Kadomtseva, V. A. Murashev, and D. N. Rakov, J. Exp. Theo. Phys. Lett. **57**, 65 (1993).
[7] A. K. Zvezdin, A. M. Kadomtseva, S. S. Krotov, A. P. Pyatakov, Yu.F. Popov, and G. P. Vorobev, J. Magn. Magn. Mater. **300**, 224 (2006).
[8] J. C. Wojdeł and J. Íñiguez, Phys. Rev. Lett. **103**, 267205 (2009).
[9] M. Mostovoy, A. Scaramucci, N. A. Spaldin, and K. T. Delaney, Phys. Rev. Lett. **105**, 087202 (2010).
[10] J. Íñiguez, Phys. Rev. Lett. **101**, 117201 (2008).
[11] J. C. Wojdeł and J. Íñiguez, Phys. Rev. Lett. **105**, 037208 (2010).
[12] S. Prosandeev, I. A. Kornev, and L. Bellaiche, Phys. Rev. B **83**, 020102 (2011).
[13] M. D. Glinchuk, A. N. Morozovska, E. A. Eliseev, and R. Blinc, J. Appl. Phys. **105**, 084108 (2009).
[14] C. W. Huang, Y. H. Chu, Z. H. Chen, J. Wang, T. Sritharan, Q. He, R. Ramesh, and L. Chen, Appl. Phys. Lett. **97**, 152901 (2010).
[15] Y. Zheng, M. Q. Cai, and C. H. Woo, Acta Mater. **58**, 3050 (2010).
[16] D. V. Karpinsky, I. O. Troyanchuk, J. V. Vidal, N. A. Sobolev, and A. L. Kholkin, Solid State Commun. **151**, 536 (2011).
[17] D. Kan, L. Pálová, V. Anbusathaiah, C. J. Cheng, S. Fujino, N. Valanoor, K. M. Rabe, and I. Takeuchi, Adv. Funct. Mater. **20**, 1108 (2010).
[18] D. A. Rusakov, A. M. Abakumov, K. Yamaura, A. A. Belik, G. Van Tendeloo, and E. Takayama-Muromachi, Chem. Mater. **23**, 285 (2011).
[19] I. O. Troyanchuk, D. V. Karpinsky, M. V. Bushinsky, V. A. Khomchenko, G. N. Kakazei, J. P. Araujo, M. Tovar, V. Sikolenko, V. Efimov, and A. L. Kholkin, Phys. Rev. B **83**, 054109 (2011).
[20] J. P. Perdew, K. Burke, and M. Ernzerhof, Phys. Rev. Lett. **77**, 3865 (1996).
[21] G. Kresse and J. Furthmuller, Phys. Rev. B **54**, 11169 (1996); G. Kresse and D. Joubert, *ibid.* **59**, 1758 (1999).
[22] O. Diéguez, O. E. González-Vázquez, J. C. Wojdeł, and J. Íñiguez, Phys. Rev. B **83**, 094105 (2011).
[23] S. L. Dudarev, G. A. Botton, S. Y. Savrasov, C. J. Humphreys, and A. P. Sutton, Phys. Rev. B **57**, 1505 (1998). We determined the value of $U = 4$ eV by requesting the computed magnetic interactions to be in quantitative agreement with those obtained from calculations with hybrid functionals. Note that $U \approx 4$ eV has become a frequent choice in first-principles studies of BFO, as it leads to qualitatively and semiquantitatively correct results for all the properties investigated so far.
[24] P. E. Blochl, Phys. Rev. B **50**, 17953 (1994); G. Kresse and D. Joubert, *ibid.* **59**, 1758 (1999).
[25] A. M. Glazer, Acta Crystallogr., Sect. B: Struct. Crystallogr. Cryst. Chem. **28**, 3384 (1972).
[26] See for example X. Wu, D. Vanderbilt, and D. R. Hamann, Phys. Rev. B **72**, 035105 (2005).
[27] Y. E. Roginskaya, Y. N. Venevtsev, S. A. Fedulov, and G. S. Zhdanov, Kristallografiya **8**, 610 (1963); Y. E. Roginskaya,

Y. N. Venevtsev, and G. S. Zhdanov, J. Exp. Theo. Phys. **44**, 1418 (1963).

[28]Z. V. Gabbasova, M. D. Kuzmin, A. K. Zvezdin, I. S. Dubenko, V. A. Murashov, D. N. Rakov, and I. B. Krynetsky, Phys. Lett. A **158**, 491 (1991).

[29]J. R. Chena, W. L. Wang, J. B. Lia, and G. H. Rao, J. Alloys Compd. **459**, 66 (2008).

[30]I. O. Troyanchuk, M. V. Bushinsky, D. V. Karpinsky, O. S. Mantytskaya, V. V. Fedotova, and O. I. Prochnenko, Phys. Status Solidi B **246**, 1901 (2009).

[31]We found that, for some Bi/La arrangements at compositions $x \lesssim 5/8$, the relaxations starting from the $O2$ structure ended up in the $O1$ phase. Analogously, for $x < 1/2$, we found cases in which relaxations starting from the $O1$ structure ended up in the $O2$ phase. These observations indicate that there are composition ranges in which the orthorhombic phases are barely stable, and in such conditions the specific Bi/La ordering becomes relevant.

[32]The quantitative values in such a hysteresis loop are not to be taken very seriously, as (i) the Landau limit for polarization switching is clearly a crude approximation to reality and (ii) the parameters of the Landau potential in Eq. (1) may vary significantly depending on the specific composition and Bi/La arrangement considered.

[33]Composition-dependent Landau theories can be found in the literature, as, for example, in the works of Haun *et al.* on the phase diagram of piezoelectric solid solution $PbZr_{1-x}Ti_xO_3$. From the series of papers published in Vol. 99 of Ferroelectrics; see, e.g., M. J. Haun, E. Furman, S. J. Jang, and L. E. Cross, Ferroelectrics **99**, 13 (1989); M. J. Haun, E. Furman, H. A. McKinstry, and L. E. Cross, *ibid.* **99**, 27 (1989).

[34]The computed parameters suggest that the PE phase would become unstable for $x' = A/\lambda = 2.85$ or, equivalently, $x = -1.85$; this negative (nonphysical) x is compatible with the fact that the $O1$ phase remains stable even in the limit of pure BFO.

[35]J. Íñiguez and L. Bellaiche, Phys. Rev. Lett. **87**, 095503 (2001); A. M. George, J. Íñiguez, and L. Bellaiche, Nature (London) **413**, 54 (2001).

[36]W. Zhong and D. Vanderbilt, Phys. Rev. Lett. **74**, 2587 (1995).

[37]Illustrative simulation results for the response properties of $KTaO_3$ at the classical (regular ferroelectric) and quantum-mechanical (incipient ferroelectric) levels can be found in A. R. Akbarzadeh, L. Bellaiche, K. Leung, J. Íñiguez, and D. Vanderbilt, Phys. Rev. B **70**, 054103 (2004).

[38]Our fitted Landau potential underestimates the strength of BFO's FE instability. For example, our potential gives an energy difference of about 150 meV/f.u. between BFO's ground state and the $P = 0$ structure, while we know from first principles that BFO's cubic PE phase lies more than 900 meV/f.u. above the R phase (Ref. 22). Such a large deviation is not totally unexpected, given that we fitted our potential to reproduce the equilibrium polarization and response properties of the FE phases, not the energy difference with respect to the cubic structure. Another consequence of this reduced stability of the FE phase is that our fitted potential renders a relatively small critical composition $x = -A/\lambda = 0.77$ at which P is predicted to disappear (see Fig. 3).

[39]E. K. H. Salje, B. Wruck, and H. Thomas, Z. Phys. B **82**, 399 (1991).

[40]I. H. Ismailzade, R. M. Ismailov, A. I. Alekberov, and F. M. Salaev, Phys. Status Solidi A **66**, 119 (1981).

[41]We have not checked the structural stability of the $Pbam$ phases and, in principle, they might be saddle points of the energy. Hence, their "metastability" is not confirmed.

[42]O. Diéguez and J. Íñiguez, Phys. Rev. Lett. **107**, 057601 (2011).

[43]J. Íñiguez, D. Vanderbilt, and L. Bellaiche, Phys. Rev. B **67**, 224107 (2003).